SolarPACES 2024, 30th International Conference on Concentrating Solar Power, Thermal, and Chemical Energy Systems

Thermal Energy Storage Materials, Media, and Systems

https://doi.org/10.52825/solarpaces.v3i.2390

Published: 11 Mar. 2026

Developing a Model for Quantifying Heat Loss From a Molten Salt Thermal Storage System

Mu-een Khan[1,*], Stephen R Clark[2], and Craig McGregor[3]

[1]Department of Mechanical and Mechatronic Engineering, Stellenbosch University, South Africa

*Correspondence: Mu-een Khan, mueenk03@gmail.com

Abstract. Thermal energy storage (TES) systems are integral to concentrated solar power (CSP) plants. A major design consideration for TES systems is the tank's storage temperature. The tank cools over time due to heat loss through its boundaries. This paper presents a model for tracking and quantifying heat loss through the tank's floor, walls, and roof. The heat transfer mechanisms incorporated in the model are convection, conduction, and radiation. The performance of the developed model is validated against previous studies and used to understand the effect of the fluid level on tank losses. The model serves as a tool to compare different thermal energy storage (TES) system designs and gain insights into which minimises the heat loss. The paper details the modelling assumptions, methodology, and validation results. The model is intended for comparative assessment during conceptual design, enabling rapid evaluation of TES configurations where relative differences matter more than absolute precision.

Keywords: Thermal Energy Storage, Heat Transfer, MATLAB/Simulink

1. Overview

TES systems increase the dispatchability of CSP plants by storing thermal energy for extended periods without significant temperature decline [1]. The cooling rate is controlled by tank insulation, and understanding heat losses can guide decisions on insulation type and thickness. The objective of the study is to develop a model to quantify heat losses from a TES tank and demonstrate its applicability to a packed-bed system. The model is intended for comparative assessment during conceptual design, enabling rapid evaluation of TES configurations where relative differences matter more than absolute precision. Figure 1 illustrates the TES tank and details the different loss streams in the system. The model development is elaborated upon in the methodology below.

2. Literature survey

A single-tank TES system utilises a thermocline to store both the hot and cold storage fluids within the same tank, rather than in separate ‘hot’ and ‘cold’ tanks. The thermocline refers to the temperature gradient separating these two temperature regions. Bonanos et al. [2] reported that heat losses to the environment result in a gradual decrease in the exit temperature of the fluid leaving the tank. Hoffman et al. [3] investigated the influence of heat loss on thermocline system efficiency and found that, during the discharge phase—when the tank is at its highest temperature—the efficiency declines more rapidly due to increased thermal losses. This aligns with fundamental heat transfer principles, as the temperature differential across the tank wall is greatest at elevated tank temperatures. Tagle-Salazar et al. [4] and Zaversky et al. [5] have

also modelled heat losses from single-tank systems, accounting for time-varying environmental conditions.

The purpose of this paper is to develop a simplified model for evaluating heat losses from a single-tank TES system. Based on the findings of Hoffman et al. [3], heat losses are modelled at the hot operating temperature to provide an upper bound on the expected losses from the TES system.

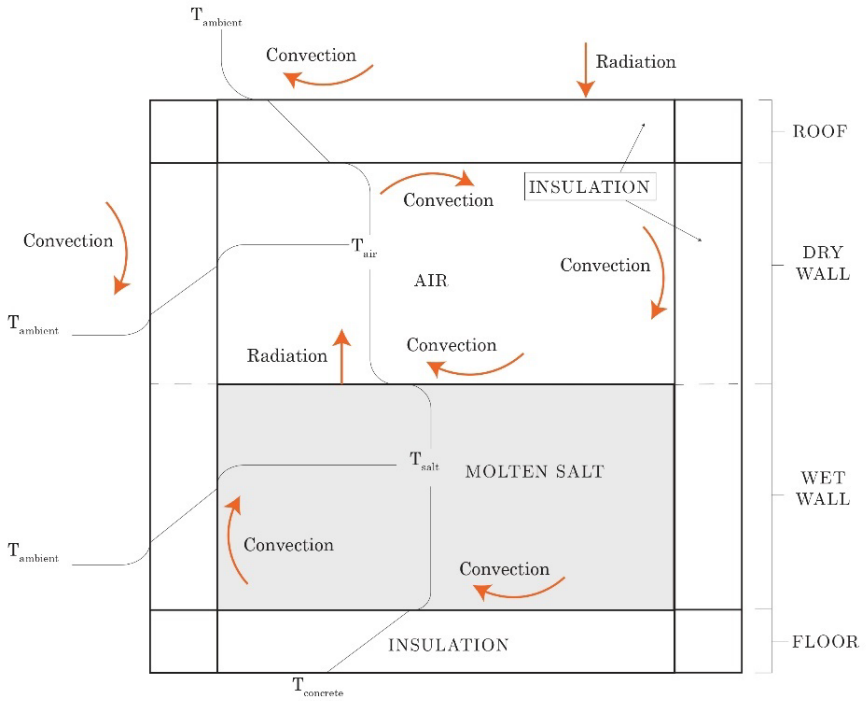

***Figure 1**. Schematic of a TES system showing the heat loss components from the molten salt*

3. Methodology

The model shown in Figure 1 illustrates a one-dimensional analysis of heat losses from the thermal energy storage system. Only the losses in the direction outward through the roof, wall, and floor are accounted for. In modelling the system, some simplifying assumptions are made. These include:

- The model assumes no mass flow into or out of the system, limiting the analysis to heat losses from the tank during its idle state.
- The molten salt is considered ideally mixed, meaning there are no temperature gradients within the fluid volume, except at the layer boundaries. This simplifies the model by representing the salt mass's temperature with a single node.
- For simplicity, the entire storage material volume is assumed to initially be at the hot temperature. This provides a conservative estimate of heat losses due to the larger temperature difference between the storage material and the outside ambient temperature.

The system uses three heat transfer mechanisms: convection, conduction and radiation. Convection occurs at the walls, the roof, the floor, and the salt-air interface. All surfaces, except the tank's external roof, are subject to natural convection. Simplifying the tank geometry, the floor, roof, and salt-air interface are modelled as flat horizontal plates. According to Tagle-Salazar et al. [4], the following two correlations have been developed to calculate the Nusselt number heat transfer coefficient for flat horizontal plates (equations 2 and 3) and a third for

vertical plates (equation 4). These relations perform better than other correlations, are valid over a wider range of Ra, Pr, and Re values, and are used in this model to determine the Nusselt numbers [6]. These Nusselt number correlations form the basis for the model being developed.

$$D \geq \frac{35L}{Gr^{1/4}} \tag{1}$$

The diameter of molten salt tanks is generally large enough that the curvature effects in the walls can be neglected. When equation 1 is satisfied, the walls can be treated as flat plates to simplify the analysis. The dimensions of commercial-scale molten salt tanks are typically less than 10 m, with a diameter of around 40 m. Finally, the external roof is subjected to forced convection and is a function of Reynold's number characterising the flow across the tank roof, governed by equation 5.

Natural convection: hot flat plate facing upwards (molten salt surface, interior roof)

$$Nu = \frac{C(Ra)^n}{\left[1+\left(\frac{0.322}{Pr}\right)^{11/20}\right]^p} \tag{2}$$

Where C=0.766, n = 1/5, P=4/11 for Ra < 10^5, and C= 0.15, n=1/3, P=20/33 for Ra > 10^5

Natural convection: cold flat plate facing upwards (floor)

$$Nu = \frac{0.667Ra^{1/5}}{\left[1+\left(\frac{0.492}{Pr}\right)^{9/16}\right]^{16/45}} \tag{3}$$

Natural convection: vertical flat plate (side walls)

$$Nu = \left[0.825 + \frac{0.387Ra^{1/6}}{\left[1+\left(\frac{0.492}{Pr}\right)^{9/16}\right]^{8/27}}\right]^2 \tag{4}$$

Mixed convection (wind over exterior roof)

$$(Nu - 0.5)^{7/2} = \left[\frac{0.677Re^{1/2}Pr^{1/3}}{\left[1+\left(\frac{0.0468}{Pr}\right)^{2/3}\right]^{1/4}}\right]^{7/2} + \left[\frac{0.76Ra^{1/5}}{\left[1+\left(\frac{0.492}{Pr}\right)^{9/16}\right]^{16/45}}\right]^{7/2} \tag{5}$$

Equation 6 describes the conduction formula used in the model. This applies to all the layers of steel and insulation making up the tank roof, wall and floor. The thickness of the tank wall, measured from the internal to the external surface is not expected to be larger than 0.5 m. In relation to the tank's 38.5~m diameter, it made sense to simplify the model by using internal dimensions to calculate the wall surface areas for the different tank layers. Where \(k\) is the thermal conductivity, \(A\) is the surface area, \(L\) is the layer thickness and \(\Delta T\) is the temperature difference across the layer.

$$q = \frac{kA}{L}\Delta T \tag{6}$$

The third mode of heat transfer is radiation. Inside the tank, radiation is emitted from the molten salt surface to the wall and roof. Outside the tank, radiation is emitted from the tank wall and roof to the sky, while simultaneously absorbing incident solar radiation. A simplified approach (equation 7) is used to compute the radiation leaving the molten salt surface. The assumption made is that the interior roof and wall are black surfaces; reflections between them

are ignored since the two surfaces are at approximately the same temperature and the focus is on the amount of radiation leaving the salt [6]. Solar radiation also affects the system. Its effect is to increase the external surface temperature and in doing so, reduce the heat loss from the tank. The Northern Cape, South Africa is the location of all the country's utility-scale CSP plants. The monthly average solar radiation for the Northern Cape is 267.38 W/m^2 [7]. This value is used along with the absorptivity of the tank jacket, to determine the irradiance. The incident solar radiation reduces overall heat losses by increasing the outside surface temperature, which in turn reduces the temperature difference across the tank wall layers.

$$\dot{Q}_i = \sum_{j=1}^{N} \dot{Q_{i \to J}} = \sum_{j=1}^{N} A_i \, F_{i \to j} \sigma \left(T_i^4 - T_j^4 \right) \tag{7}$$

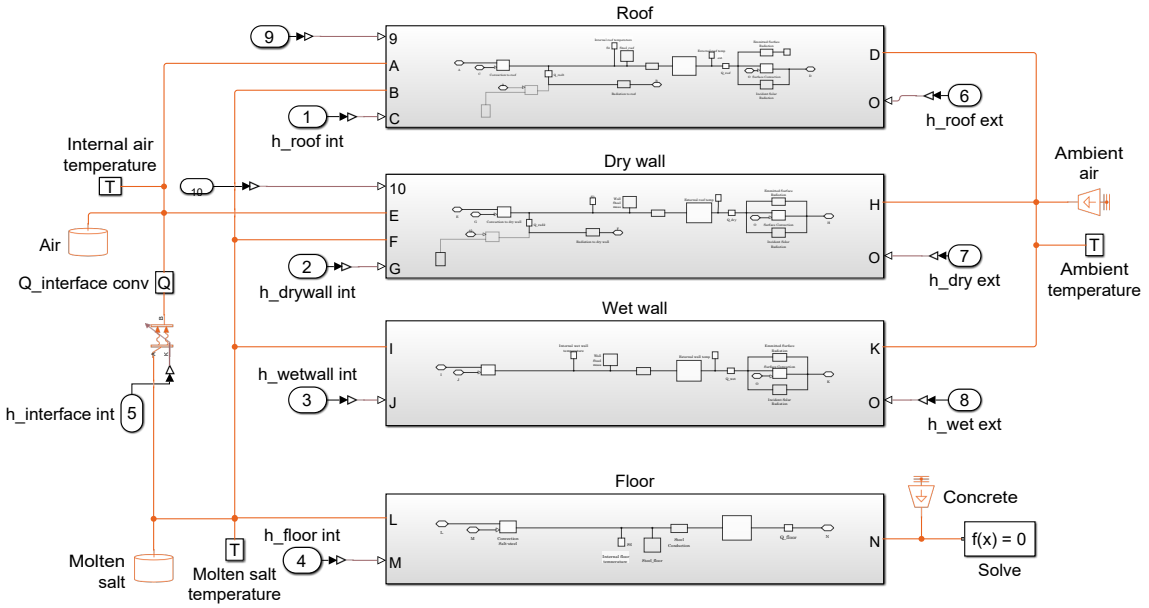

***Figure 2**. Simulink model showing the whole TES system*

The model was implemented in MATLAB/Simulink using the Simscape thermal elements package [8]. Simulink is a graphical modelling tool that facilitates the visualisation of the physical system. Figure 2 shows the model in the Simulink environment. Each labelled subsystem represents the heat transfer through the different areas of the tank.

4. Validation and results

Studies by Tagle-Salazar et al. [4] and Zaversky et al. [5] have been identified which developed very similar models for molten salt storage tanks. This study will serve as a reference for validating the model. Table 1 lists the parameters used in the study to define the system.

The tank wall and roof are composed of an inner stainless-steel layer and an outer thermal-insulation layer. Finally, a thin layer of galvanised steel covers the insulation. The floor consists of an inner layer of stainless steel, a thermal insulation layer, and a concrete layer. In conventional designs, the concrete layer is air-cooled through a channel exposed to the atmosphere, maintaining the concrete temperature below 90 °C. This is implemented as a 90 °C temperature boundary at the concrete-insulation interface.

Time-varying variables such as solar irradiance and wind speed are simplified by averaging them over time. Salt and air properties inside the tank are calculated at the hot temperature, while ambient temperature air properties are used external to the tank. Thermal conductivities in the model vary with temperature.

Table 1. *Inputs to the model*

Model inputs		**Unit**	**Value**
Diameter		m	38.5
Height		m	14
Full/Empty level		m	13/0.7
Temperature	Hot/Cold	°C	565/290
Shell thickness	Roof	mm	6
	Wall/Floor	mm	4
Insulation type	Roof	-	Calcium silicate
	Wall	-	Mineral wool
	Floor	-	Foamglas
Insulation thicknesses		m	0.4
Ambient air temperature		°C	22.4
Effective sky temperature		°C	0
Concrete temperature		°C	90
Insulation jacket material		-	Galvanised steel
Effective wind speed		m/s	4.35
Effective solar irradiance		W/m^2	267

Figure 3 shows the heat loss components at different tank salt levels. These results were recorded on the second simulation day to avoid the transient behaviour associated with start-up conditions on the first day. Table 2 compares the results of this model with those developed by Tagle-Salazar et al. [4] and Zaversky et al. [5]. The model's design inputs match those used in the reference studies, enabling a direct comparison of outputs.

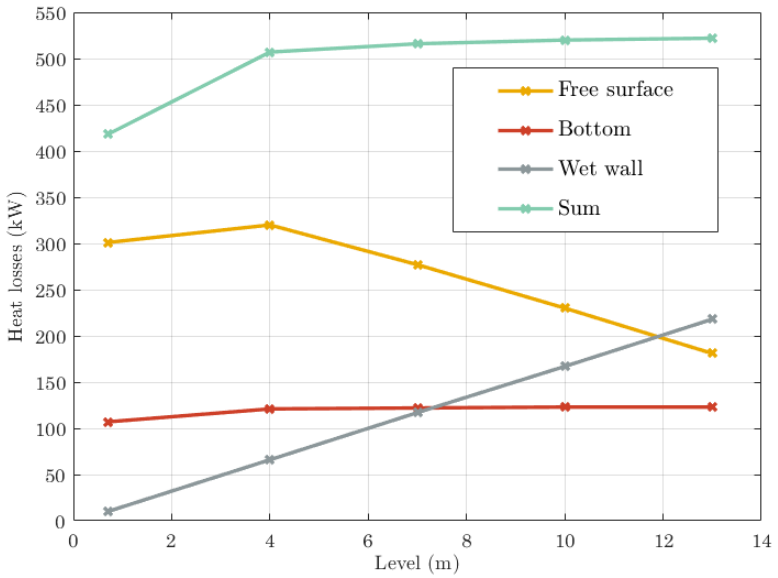

Figure 3. *Heat losses at various tank fill levels*

The table lists the heat losses recorded by the reference studies and those calculated using this model. The errors, calculated by equation 8 are reported alongside. The first error column reports the error, normalised with the respective heat loss component. Doing so does not account for the loss component's contribution to total losses, and hence some small components can contribute to large percentage errors. The relative scale of the components can be accounted for by normalising the error with respect to the total heat loss. The errors are reported in the last column. All the heat losses are within 10% of the reference studies. This level of accuracy is considered satisfactory for estimating heat losses from a storage tank. For

research purposes, it is sufficient to compare different concepts rather than accurately account for all the heat lost from the system.

$$\%\ \text{error} = \frac{(\text{Model} - \text{Reference})}{\text{Reference}} \cdot 100\% \tag{8}$$

Table 2. *A comparison of the heat loss results obtained*

Salt level	Component	References [kW] [2] [3]	This model [kW]	% error normalised by component heat loss	% error normalised by total heat loss
Full	Surface radiation	180	163	-6	-2
	Surface convection	5	18	140	1
	Wall convection	195	218	12	5
	Floor convection	110	123	12	3
	Total heat loss	**490**	**523**	**7**	**7**
Empty	Surface radiation	285	285	0	0
	Surface convection	6	16	167	3
	Wall convection	9	10	11	0
	Floor convection	80	107	34	7
	Total heat loss	**380**	**418**	**10**	**10**

The model shows fair agreement with the reference studies. The model does use a few simplifications: constant environmental parameters, a simplified radiation model for the tank's internal surfaces, and a constant temperature profile throughout the molten salt in the tank. To support the use of constant environmental parameters such as wind speed, solar irradiance, and ambient temperature, a sensitivity analysis was performed to quantify the influence of each variable on the system heat losses. The results are summarised in Table 3 below. Over the ranges investigated, the effect of each parameter on heat loss did not exceed 2%, confirming the approach and supporting the simplification. To estimate heat losses during the early feasibility and conceptual phases of design projects, the model provides efficient insight into the capabilities of thermal energy storage systems. For detailed design where accurate heat losses and efficiencies are desired, a more refined model that revisits the simplifications made should be implemented. This, however, is beyond the focus of this study.

Table 3. *Sensitivity analysis*

Parameter	Unit	Value	Total heat loss (kW)	% from baseline
Baseline	-	-	523	-
Ambient temp	°C	5	534	2%
		40	512	2%
Wind speed	m/s	2	523	0%
		12	523	0%
Irradiance	W/m²	0	527	1%
		800	514	2%

5. Case study: heat loss from a packed bed

The model developed in the previous section was validated for a standard molten salt tank. In this section, we present a case study that applies the model to a packed-bed TES system. A packed-bed tank should be much larger to achieve the same thermal storage capacity as the previously explored molten salt tank. This is because the volumetric heat capacity of clay-based bricks is approximately 1 MJ/m^{3}K less than that of molten salt [9]. The increased tank size translates into a larger surface area through which heat is lost from the tank. The tank

investigated in the previous section is based on the Andasol CSP plant and is designed to supply power to a power block rated at 150 MWe for 7.5 hours [10]. A packed bed tank with an equivalent thermal storage capacity and a void fraction of 0.2 will need to be 14 m high by 58 m in diameter.

With a packed bed tank, the boundary conditions at the wet walls and the floor change. There is no longer a convection boundary as with the standard molten salt case. Instead, the bricks are now in contact with the internal tank walls, and heat is transferred via conduction. In modelling the packed bed here, the complex heat transfer behaviour between the packed bed and the molten salt is modelled as a lumped mass with uniform temperature to simplify the analysis. This is implemented as a temperature boundary at the tank interior wall and floor. This conservative assumption is appropriate for insulation sizing applications, where the design must accommodate the maximum heat flux condition that occurs when hot storage material contacts the tank boundaries.

Table 4 lists the heat losses for a packed-bed TES system alongside the previously obtained results for a standard molten-salt TES system. Under the conservative uniform-temperature assumption, the packed bed system's upper-bound heat loss is approximately 70% higher than the molten salt tank with equivalent storage capacity. This increase is primarily attributable to the larger surface area required (58 m vs 38.5 m diameter) to compensate for the lower volumetric heat capacity of the packed bed material. Measures to reduce heat loss, such as increased insulation thickness, should be considered during detailed design.

Table 4. *Comparison of heat losses between standard molten salt and a packed bed tank*

Component	**Standard molten salt tank heat loss [kW]**	**Packed bed tank heat loss [kW]**
Surface (radiation)	163	363
Surface (convection)	18	20
Wall (conduction)	218	276
Floor	123	235
Total	**523**	**893**

6. Conclusion

The model was developed and shows reasonable agreement with published results for a two-tank molten salt system under steady-state conditions. A sensitivity analysis confirmed that time-varying ambient conditions affect total heat loss by no more than 2%, supporting the use of representative average values. The model is suitable for comparative assessment of TES configurations during conceptual design. Its application to a packed-bed system was demonstrated, with the conservative uniform-temperature assumption providing an upper bound on heat losses suitable for insulation sizing.

Data availability statement

Data is available on request.

Author contributions

Mu-een Khan: conceptualisation, software, methodology, validation, visualisation, writing - original draft. Stephen R Clark: writing - review \& editing. Craig McGregor: supervision, conceptualisation, writing - review \& editing, resources.

Competing interests

The authors declare that they have no competing interests.

Funding

The authors acknowledge the financial support of the Solar Thermal Energy Research Group (STERG) at Stellenbosch University.

Acknowledgement

I want to express my gratitude to STERG, its researchers and support staff for their continuous support.

References

[1] C. Prieto, P. D. Tagle-Salazar, D. Patino, J. Schallenberg-Rodriguez, P. Lyons, and L. F. Cabeza, “Use of molten salts tanks for seasonal thermal energy storage for high penetration of renewable energies in the grid,” Journal of Energy Storage, vol. 86, p. 111 203, 2024. DOI: 10.1016/j.est.2024.111203.

[2] Bonanos, A.M. and Votyakov, E.V., 2021. Analysis of thermocline thermal energy storage systems with generic initial condition algebraic model. *Solar Energy*, *213*, pp.154-162. DOI: 10.1016/j.solener.2020.11.011

[3] Hoffmann, J.F., Fasquelle, T., Goetz, V. and Py, X., 2017. Experimental and numerical investigation of a thermocline thermal energy storage tank. Applied Thermal Engineering, 114, pp.896-904. DOI: 10.1016/j.applthermaleng.2016.12.053

[4] P. D. Tagle-Salazar, C. Prieto, A. L ´opez-Rom ´an, and L. F. Cabeza, “A transient heat losses model for two-tank storage systems with molten salts,” Renewable Energy, vol. 219, p. 119 371, 2023. DOI: 10.1016/j.renene.2023.119371.

[5] F. Zaversky, J. Garc´ıa-Barberena, M. S ´anchez, and D. Astrain, “Transient molten salt two-tank thermal storage modeling for csp performance simulations,” Solar Energy, vol. 93, pp. 294–311, 2013. DOI: 10.1016/j.solener.2013.02.034.

[6] Y. A. C¸ engel, A. J. Ghajar, and M. Kanoglu, Heat and mass transfer: Fundamentals and applications. McGraw-Hill, 2011, ISBN: 978-007-131112-0.

[7] J. Singh, “Ranking south african provinces on the basis of merra 2d surface incident shortwave flux,” Journal of Energy in Southern Africa, vol. 27, no. 3, pp. 50–57, 2016, Irradiance in northern cape, ISSN: 2413-3051.

[8] The MathWorks, Inc., Simscape, [Online; accessed Aug 2024], Aug. 2024. [Online]. Available: https://www.mathworks.com/products/simscape.html.

[9] L. Snyman and C. McGregor, “Ceramic composite structured packing for cost-effective thermal energy storage in concentrating solar power plants,” Mar. 2024, Liam Snyman research. (visited on 12/05/2024).

[10] F. Dinter and D. M. Gonzalez, “Operability, reliability and economic benefits of csp with thermal energy storage: First year of operation of andasol 3,” Energy Procedia, vol. 49, pp. 2472–2481, 2014. DOI: 10.1016/j.egypro.2014.03.262.